

REPORT DOCUMENTATION PAGE			Form Approved OMB NO. 0704-0188		
<p>The public reporting burden for this collection of information is estimated to average 1 hour per response, including the time for reviewing instructions, searching existing data sources, gathering and maintaining the data needed, and completing and reviewing the collection of information. Send comments regarding this burden estimate or any other aspect of this collection of information, including suggestions for reducing this burden, to Washington Headquarters Services, Directorate for Information Operations and Reports, 1215 Jefferson Davis Highway, Suite 1204, Arlington VA, 22202-4302. Respondents should be aware that notwithstanding any other provision of law, no person shall be subject to any penalty for failing to comply with a collection of information if it does not display a currently valid OMB control number.</p> <p>PLEASE DO NOT RETURN YOUR FORM TO THE ABOVE ADDRESS.</p>					
1. REPORT DATE (DD-MM-YYYY) 09-12-2014		2. REPORT TYPE Final Report		3. DATES COVERED (From - To) 1-Aug-2009 - 31-Jul-2014	
4. TITLE AND SUBTITLE Final Report: A Multi-Scale Modeling and Experimental Program for the Dynamic Mechanical Response of Tissue			5a. CONTRACT NUMBER W911NF-09-1-0378		
			5b. GRANT NUMBER		
			5c. PROGRAM ELEMENT NUMBER 8D10AZ		
6. AUTHORS Jay Schieber, David Gidalevitz, Joseph Orgel, Victor Perez-Luna			5d. PROJECT NUMBER		
			5e. TASK NUMBER		
			5f. WORK UNIT NUMBER		
7. PERFORMING ORGANIZATION NAMES AND ADDRESSES Illinois Institute of Technology 3300 South Federal Street Room 301 Main Bldg Chicago, IL 60616 -3793			8. PERFORMING ORGANIZATION REPORT NUMBER		
9. SPONSORING/MONITORING AGENCY NAME(S) AND ADDRESS (ES) U.S. Army Research Office P.O. Box 12211 Research Triangle Park, NC 27709-2211			10. SPONSOR/MONITOR'S ACRONYM(S) ARO		
			11. SPONSOR/MONITOR'S REPORT NUMBER(S) 56388-EG-DRP.42		
12. DISTRIBUTION AVAILABILITY STATEMENT Approved for Public Release; Distribution Unlimited					
13. SUPPLEMENTARY NOTES The views, opinions and/or findings contained in this report are those of the author(s) and should not be construed as an official Department of the Army position, policy or decision, unless so designated by other documentation.					
14. ABSTRACT We study the mechanical properties of collagen, which is the most prevalent protein in humans, and largely responsible for the mechanical properties of tissue. We use both a multiscale modeling approach, and experiments to examine the theoretical results. The atomistic structure of collagen is determined by X-ray diffraction, which provides the starting point for atomistic simulations. These simulations are then used to predict the modulus of collagen fibrils. The bending modulus of fibrils is finally measured by using optical tweezers.					
15. SUBJECT TERMS collagen, multiscale modeling, mechanics, modulus, rheology					
16. SECURITY CLASSIFICATION OF:			17. LIMITATION OF ABSTRACT	15. NUMBER OF PAGES	19a. NAME OF RESPONSIBLE PERSON
a. REPORT UU	b. ABSTRACT UU	c. THIS PAGE UU			Jay Schieber
					19b. TELEPHONE NUMBER 312-567-3046

Report Title

Final Report: A Multi-Scale Modeling and Experimental Program for the Dynamic Mechanical Response of Tissue

ABSTRACT

We study the mechanical properties of collagen, which is the most prevalent protein in humans, and largely responsible for the mechanical properties of tissue. We use both a multiscale modeling approach, and experiments to examine the theoretical results. The atomistic structure of collagen is determined by Xray diffraction, which provides the starting point for atomistic simulations. These simulations are then used to predict the modulus of collagen fibrils. The bending modulus of fibrils is finally measured by using optical tweezers.

Enter List of papers submitted or published that acknowledge ARO support from the start of the project to the date of this printing. List the papers, including journal references, in the following categories:

(a) Papers published in peer-reviewed journals (N/A for none)

<u>Received</u>	<u>Paper</u>
08/31/2012 11.00	D. M. Rogers, S. Varma, L. R. Pratt, S. B. Rempe. Perspectives on: Ion selectivity: Design principles for K ⁺ selectivity in membrane transport, <i>Journal of General Physiology</i> , (05 2011): 479. doi: 10.1085/jgp.201010579
08/31/2012 23.00	Rudi J. A. Steenbakkers, Jay D. Schieber. Derivation of free energy expressions for tube models from coarse-grained slip-link models, <i>The Journal of Chemical Physics</i> , (07 2012): 34901. doi: 10.1063/1.4730170
08/31/2012 21.00	Andres Cordoba, Jay D. Schieber, Tsutomu Indei. The effects of hydrodynamic interaction and inertia in determining the high-frequency dynamic modulus of a viscoelastic fluid with two-point passive microrheology, <i>Physics of Fluids</i> , (07 2012): 73103. doi: 10.1063/1.4734388
08/31/2012 20.00	Andrés Córdoba, Tsutomu Indei, Jay D. Schieber. Elimination of inertia from a Generalized Langevin Equation: Applications to microbead rheology modeling and data analysis, <i>Journal of Rheology</i> , (01 2012): 185. doi: 10.1122/1.3675625
08/31/2012 19.00	Tsutomu Indei, Jay Schieber, Andrés Córdoba, Ekaterina Pilyugina. Treating inertia in passive microbead rheology, <i>Physical Review E</i> , (02 2012): 21504. doi: 10.1103/PhysRevE.85.021504
08/31/2012 18.00	Tsutomu Indei, Jay Schieber, Andrés Córdoba. Competing effects of particle and medium inertia on particle diffusion in viscoelastic materials, and their ramifications for passive microrheology, <i>Physical Review E</i> , (04 2012): 41504. doi: 10.1103/PhysRevE.85.041504
08/31/2012 17.00	Andrey Ivankin, Liran Livne, Amram Mor, Gregory A. Caputo, William F. DeGrado, Mati Meron, Binhua Lin, David Gidalevitz. Role of the Conformational Rigidity in the Design of Biomimetic Antimicrobial Compounds, <i>Angewandte Chemie International Edition</i> , (11 2010): 8462. doi: 10.1002/anie.201003104
08/31/2012 16.00	Beatriz Apellániz, Andrey Ivankin, Shlomo Nir, David Gidalevitz, José L. Nieva. Membrane-Proximal External HIV-1 gp41 Motif Adapted for Destabilizing the Highly Rigid Viral Envelope, <i>Biophysical Journal</i> , (11 2011): 0. doi: 10.1016/j.bpj.2011.10.005
08/31/2012 15.00	Andrey Ivankin, Ivan Kuzmenko, David Gidalevitz. Cholesterol Mediates Membrane Curvature during Fusion Events, <i>Physical Review Letters</i> , (06 2012): 238301. doi: 10.1103/PhysRevLett.108.238103
08/31/2012 12.00	J. P. R. O. Orgel, O. Antipova, I. Sagi, A. Bitler, D. Qiu, R. Wang, Y. Xu, J. D. San Antonio. Collagen fibril surface displays a constellation of sites capable of promoting fibril assembly, stability, and hemostasis, <i>Connective Tissue Research</i> , (02 2011): 18. doi: 10.3109/03008207.2010.511354
09/07/2011 3.00	David C. Venerus, Teresita Kashyap. Stress Relaxation in Polymer Melts Following Equibiaxial Step Strain, <i>Macromolecules</i> , (07 2010): 0. doi: 10.1021/ma100689y
09/07/2011 13.00	O. Antipova, J. P. R. O. Orgel. In Situ D-periodic Molecular Structure of Type II Collagen, <i>Journal of Biological Chemistry</i> , (01 2010): 7087. doi: 10.1074/jbc.M109.060400

- 09/07/2011 8.00 Renat N. Khaliullin, Jay D. Schieber. Calculation of the Helmholtz potential of an elastic strand in an external electric field, *The Journal of Chemical Physics*, (02 2011): 65105. doi: 10.1063/1.3532830
- 09/07/2011 7.00 Renat N. Khaliullin, Jay D. Schieber. Application of the Slip-Link Model to Bidisperse Systems, *Macromolecules*, (07 2010): 6202. doi: 10.1021/ma902823k
- 09/07/2011 6.00 Kazushi Horio, Jay D. Schieber. Fluctuation in entanglement positions via elastic slip-links, *The Journal of Chemical Physics*, (02 2010): 74905. doi: 10.1063/1.3314727
- 09/08/2011 10.00 Mette Krog Jensen, Renat Khaliullin, Jay D. Schieber. Self-consistent modeling of entangled network strands and linear dangling structures in a single-strand mean-field slip-link model, *Rheologica Acta*, (7 2011): 0. doi: 10.1007/s00397-011-0568-8
- 09/24/2013 24.00 Andrés Córdoba, Tsutomu Idei, Jay D. Schieber. The effects of compressibility, hydrodynamic interaction and inertia on two-point, passive microrheology of viscoelastic materials, *Soft Matter*, (02 2013): 3521. doi: 10.1039/c3sm27266d
- 09/24/2013 14.00 Beatriz Apellániz, David Gidalevitz, Andrey Ivankin, José L. Nieva. Mechanism of membrane perturbation by the HIV-1 gp41 membrane-proximal external region and its modulation by cholesterol, *Biochimica et Biophysica Acta (BBA) - Biomembranes*, (11 2012): 2521. doi: 10.1016/j.bbamem.2012.06.002
- 09/24/2013 25.00 Tsutomu Idei, Jay D. Schieber, Andrés Córdoba. The analytic solution of Stokes for time-dependent creeping flow around a sphere: Application to linear viscoelasticity as an ingredient for the generalized Stokes–Einstein relation and microrheology analysis, *Journal of Non-Newtonian Fluid Mechanics*, (10 2013): 3. doi: 10.1016/j.jnnfm.2012.08.002
- 11/19/2014 26.00 Cédric Zeltz, Joseph Orgel, Donald Gullberg. Molecular composition and function of integrin-based collagen glues—Introducing COLINBRIs, *Biochimica et Biophysica Acta (BBA) - General Subjects*, (08 2014): 2533. doi: 10.1016/j.bbagen.2013.12.022
- 11/19/2014 27.00 Joseph P. R. O. Orgel, Anton V. Persikov, Olga Antipova, Collin M. Stultz. Variation in the Helical Structure of Native Collagen, *PLoS ONE*, (02 2014): 89519. doi: 10.1371/journal.pone.0089519
- 11/19/2014 28.00 Konstantin Andreev, Christopher Bianchi, Jonas S. Laursen, Linda Citterio, Line Hein-Kristensen, Lone Gram, Ivan Kuzmenko, Christian A. Olsen, David Gidalevitz. Guanidino groups greatly enhance the action of antimicrobial peptidomimetics against bacterial cytoplasmic membranes, *Biochimica et Biophysica Acta (BBA) - Biomembranes*, (10 2014): 2492. doi: 10.1016/j.bbamem.2014.05.022
- 11/19/2014 29.00 Andrés Córdoba, Jay D. Schieber, Tsutomu Idei. A single-chain model for active gels I: active dumbbell model, *RSC Advances*, (03 2014): 17935. doi: 10.1039/c4ra02262a
- 11/19/2014 30.00 Tsutomu Idei, Jay D. Schieber. Correction of Doi-Edwards' Green function for a chain in a harmonic potential and its implication for the stress-optic rule, *Journal of Polymer Science Part B: Polymer Physics*, (03 2014): 460. doi: 10.1002/polb.23439
- 11/19/2014 31.00 Maria Katzarova, Marat Andreev, Yelena R. Sliozberg, Randy A. Mrozek, Joseph L. Lenhart, Jan W. Andzelm, Jay D. Schieber. Rheological predictions of network systems swollen with entangled solvent, *AIChE Journal*, (04 2014): 1372. doi: 10.1002/aic.14370

TOTAL: 25

Number of Papers published in peer-reviewed journals:

(b) Papers published in non-peer-reviewed journals (N/A for none)

Received

Paper

08/31/2012 22:00 Jay D. Schieber, Andres Cordoba, Tsutomu Indei. The analytic solution of Stokes for time-dependent creeping flow around a sphere: application to linear viscoelasticity as an ingredient for the Generalized Stokes-Einstein relation and microrheology analysis., Journal of Non-Newtonian Fluid Mechanics, (11 2012): 0. doi:

TOTAL: 1

Number of Papers published in non peer-reviewed journals:

(c) Presentations

(1) 8 October 2014, Stanford University, Palo Alto, California, "Diffusion and Microrheology in Viscoelastic Media: Effects of Inertia and Non-Conservative Force" (JDS, Tsutomu Indei and Andrés Córdoba)

(2) 27 September 2013, University of Western Michigan, Department of Paper Engineering, Chemical Engineering and Imaging, "Diffusion and Microrheology in Viscoelastic Media: Effects of Inertia and Non-Conservative Forces"

(3) March 05, 2014, American Physical Society Meeting, Inertial effects in viscoelastic materials and their implication in passive microrheology" Tsutomu Indei, Jay D Schieber, Andrés Córdoba

(4) March 06, 2014, American Physical Society Meeting, "Calibration of optical traps by dual trapping of one bead" Pavel Dutov, Jay D Schieber

(5) October 14, 2013, Society of Rheology Annual Meeting, "Limitation in single-bead passive microrheology" Tsutomu Indei

(6) "Recent progress in X-ray diffraction based studies of amyloid, prion and fibril based brain diseases". Speaker, Session Chair of Pathological Fibrils, American Crystallographic Association, Albuquerque NM, May 2014. Joseph Orgel

(7) "Molecular Structure and Organization of the Collagens whilst in their Tissues as Shown by X-ray Diffraction". Speaker, Session Chair of Flesh and Blood, American Crystallographic Association, Albuquerque NM, May 2014. Joseph Orgel

(8) "Experimentally Determined Molecular Structure and Organization of Collagen in Tissues". Podium presentation, World Congress of Biomechanics, Boston MA, May 2014. Joseph Orgel

(9) "Type I collagen molecular map lends insights into the domain structure of the fibril and the genotype-phenotype relationship for some collagen mutations." Podium Talk. 12th International Conference on Osteogenesis Imperfecta, October 12-15, 2014. Joseph Orgel

(10) "Visualization challenges for biomedical research". Invited talk at the department of Biomedical Illustration and Visualization, UIC, (2014). Joseph Orgel

(11) "How Collagen Structure and Remodelling Influences Cellular Interaction". Invited talk at NIH main campus, Biophysics and Structural Biology Series, Nov 2014. Joseph Orgel

Number of Presentations: 11.00

Non Peer-Reviewed Conference Proceeding publications (other than abstracts):

<u>Received</u>	<u>Paper</u>
11/19/2014 35.00	Jay Schieber, Andres Cordoba, Tsutomu Indei. Diffusion and Microrheology in Viscoelastic Media: Effects of Inertia and Non-Conservative Forces, European Condensed Matter Physics in Paris. 25-AUG-14, . : ,
11/19/2014 32.00	Andres Cordoba, Jay Schieber. A Single-Chain Model to Predict Buckling in Active Gels, Biophysical Society. 16-FEB-14, . : ,
11/19/2014 33.00	Pavel Dutoy, Jay D. Schieber, Olga Antipova , Sameer Varma, Joseph Orgel. Collagen Single Fibril Elastic Modulus Measurement Technique, Biophysical Society. 19-FEB-14, . : ,
11/19/2014 34.00	Jay Schieber, Andres Cordoba, Tsutomu Indei. A Single-Chain Model to Predict Buckling in Active Gels, World Congress on Biomechanics. 07-JUL-14, . : ,
11/19/2014 37.00	Tsutomu Indei, Jay Schieber, Andres Cordoba. Inertial effects in viscoelastic materials and their implication in passive microrheology, American Physical Society. 05-MAR-14, . : ,
11/19/2014 38.00	Pavel Dutoy, Jay Schieber. Calibration of optical traps by dual trapping of one bead, American Physical Society. 06-MAR-14, . : ,
TOTAL:	6

Number of Non Peer-Reviewed Conference Proceeding publications (other than abstracts):

Peer-Reviewed Conference Proceeding publications (other than abstracts):

<u>Received</u>	<u>Paper</u>
-----------------	--------------

TOTAL:

Number of Peer-Reviewed Conference Proceeding publications (other than abstracts):

(d) Manuscripts

Received

Paper

11/19/2014 40.00 Pavel Dutoy, Olga Antipova, Sameer Varma , Joseph Orgel, Jay Schieber. Measurement of Elastic Modulus of Collagen Type I Single Fiber, Biophysical Journal (10 2014)

11/19/2014 39.00 Sameer Varma, Mohsen Botlani, Jeff R. Hammond, Paul Tumaneng, H. Larry Scott, Joseph P. R. O. Orgel, Jay Schieber. Nanomechanics of type Icollagen fibrils, (09 2014)

TOTAL: 2

Number of Manuscripts:

Books

Received

Book

TOTAL:

Received

Book Chapter

11/19/2014 36.00 Joseph Orgel, Tom Irving. Encyclopedia of Analytical Chemistry, Chichester, UK: John Wiley & Sons, Ltd, (06 2014)

TOTAL: 1

Patents Submitted

Patents Awarded

Awards

Graduate Students

<u>NAME</u>	<u>PERCENT SUPPORTED</u>	Discipline
Junjun Zhang	1.00	
Pavel Dutov	1.00	
Konstantin Andreev	1.00	
FTE Equivalent:	3.00	
Total Number:	3	

Names of Post Doctorates

<u>NAME</u>	<u>PERCENT SUPPORTED</u>
FTE Equivalent:	
Total Number:	

Names of Faculty Supported

<u>NAME</u>	<u>PERCENT SUPPORTED</u>	National Academy Member
Jay Schieber	0.20	No
Sameer Varma	0.09	
FTE Equivalent:	0.29	
Total Number:	2	

Names of Under Graduate students supported

<u>NAME</u>	<u>PERCENT SUPPORTED</u>
FTE Equivalent:	
Total Number:	

Student Metrics

This section only applies to graduating undergraduates supported by this agreement in this reporting period

The number of undergraduates funded by this agreement who graduated during this period: 0.00

The number of undergraduates funded by this agreement who graduated during this period with a degree in science, mathematics, engineering, or technology fields:..... 0.00

The number of undergraduates funded by your agreement who graduated during this period and will continue to pursue a graduate or Ph.D. degree in science, mathematics, engineering, or technology fields:..... 0.00

Number of graduating undergraduates who achieved a 3.5 GPA to 4.0 (4.0 max scale):..... 0.00

Number of graduating undergraduates funded by a DoD funded Center of Excellence grant for Education, Research and Engineering:..... 0.00

The number of undergraduates funded by your agreement who graduated during this period and intend to work for the Department of Defense 0.00

The number of undergraduates funded by your agreement who graduated during this period and will receive scholarships or fellowships for further studies in science, mathematics, engineering or technology fields:..... 0.00

Names of Personnel receiving masters degrees

NAME

Total Number:

Names of personnel receiving PHDs

NAME

Total Number:

Names of other research staff

NAME

PERCENT SUPPORTED

FTE Equivalent:

Total Number:

Sub Contractors (DD882)

1 a. University of South Florida at Tampa

1 b. 3702 Spectrum Blvd

Suite 165

Tampa

FL

336129445

Sub Contractor Numbers (c):

Patent Clause Number (d-1):

Patent Date (d-2):

Work Description (e): We will carry out explicit solvent molecular dynamics simulations of the collagen Type-I

Sub Contract Award Date (f-1):

Sub Contract Est Completion Date(f-2):

1 a. University of South Florida at Tampa

1 b. 4202 East Fowler Avenue, FAO126

Tampa

FL

336207900

Sub Contractor Numbers (c):

Patent Clause Number (d-1):

Patent Date (d-2):

Work Description (e): We will carry out explicit solvent molecular dynamics simulations of the collagen Type-I

Sub Contract Award Date (f-1):

Sub Contract Est Completion Date(f-2):

Inventions (DD882)**Scientific Progress**

See Attachment

Technology Transfer

DARPA Scientific Progress Report, 2014

We seek to predict the mechanical properties of human tissue from atomistic simulations and microrheological experiments. The most prevalent protein in the body is also one that determines much of its mechanical properties: collagen. Collagen is a multiscale material, so requires multiscale modeling for predictions. It consists of long proteins that form a triple helix. The triple helices stack to form fibrils of a few hundred nanometers in diameter. In turn, these fibrils then bind to form fibers that have the important mechanical strength. We show that the modulus of the triple helix and fibrils are very similar, but that the fibers have much lower modulus. Hence, we postulate that the inter-fibril cross-linking is significantly softer than collagen. Details are in the submitted manuscript *Nanomechanics of type I collagen fibrils*, and only a brief summary is given below.

Our overall strategy is the following steps. Co-principal investigator Joseph Orgel has performed x-ray diffraction to determine the atomistic structure of the stacking in the fibrils. These structures are then fed into an atomistic molecular dynamics simulation. Many of the force fields between atoms are determined from *ab initio* quantum mechanical calculations, and these are then used to determine the stresses in the fibril material as function of strain. The simulations use periodic boundary conditions to assume that the fibrils are infinitely large. The results of the simulation are used to determine parameters in a linear elastic rod model. These predictions are compared to single-fiber mechanical measurements performed using optical tweezers (see manuscript “Measurement of elastic modulus of collagen Type I single fiber”). Finally, microrheology is performed on gels made of collagen. Most details are given in previous reports, published papers and proceedings, all of which are included elsewhere in the report. In the following sections we focus here on what is new and not in those other publications.

We also examine the properties of oriented and unoriented gels. We have developed techniques to quantify the anisotropy of the gel, whose structure was created by periodic deformations during crosslinking. We also show that two-point microrheology can be used to measure the modulus of gels whose microstructure is larger than bead size. These details are given below.

Molecular dynamics simulation

Collagen is the primary constituent of animal connective tissue. A defining feature of fibrillar collagen is its axial periodicity visible in transmission electron microscopy as alternating dark and light bands. The repeating unit, D, is 67 nm long, with the dark band making up 54% of the repeating length. This periodicity of dark/light bands reflects an underlying packing of constituent triple-helix polypeptide monomers wherein the dark bands represent gaps between axially adjacent monomers. This organization of gap/overlap regions is present in the microfibrillar model of collagen obtained from fiber diffraction at 55 Angstrom resolution.

Recent molecular dynamics simulations of this model under zero-stress conditions, however, predict that the D-band shrinks by 19% [1]. Consequently, the mechanical properties obtained from this study correspond to those of distorted microfibrils. Here we evaluate systematically the effect of several physical parameters on D-band shrinking. Using the force field employed in the reported study, we find that, irrespective of the temperature/pressure coupling algorithms, assumed salt concentration or hydration level, and whether or not the monomers are cross-linked, the D-band shrinks considerably. This shrinkage

results not from the sliding of axially parallel monomers across one another, but rather it is associated with bending and widening of individual monomers. The distributions of backbone dihedrals are also different from those in the fiber diffraction model.

Employing a force field whose backbone dihedral energy landscape matches more closely with CCSD(T) theory results in a small D-band shrinking of <3%. Since this force field is also known to perform better against other experimental structural data, it appears that the large shrinkage observed in earlier simulations is a force-field artifact. However, certain atomic-level details, like glycosylation sites, which are indiscernible from the electron densities of collagen and collagen-related peptides, still remain to be incorporated into the atomically detailed model of collagen. It is, therefore, plausible that their inclusion might prevent large force-field-dependent variations in D-band length. Consequently, we cannot yet completely rule out D-band shrinking to be an artifact of model construction.

Fibrils of type I collagen assemble from polypeptide triple helices. Higher-order structures, such as fibril-bundles and fibers, assemble from fibrils in the presence of other collagenous and non-collagenous molecules. A compilation of results from several different experiments indicates that the Young's moduli of fibrils/fibril-bundles are an order in magnitude smaller than those of triple helices, indicating that fibrils/fiber-bundles are less resistant to axial deformation compared to triple helices. To understand the molecular basis for this difference, we carry out all-atom molecular dynamics simulations of the smallest repeating crystallographic unit of a fibril under periodic boundary conditions. This system is structurally equivalent to an infinite microfibril. Assuming that linear response theory applies to axial strains smaller than 5%, we find that the stress-strain relationship yields a Young's modulus of 2.34 GPa, which is within the range estimated for triple helices. This similar magnitude in modulus suggests that the smaller resistance of collagen fibrils/fiber-bundles to axial deformation does not stem from the packing of polypeptide triple helices in a microfibril. Instead, it stems from the assembly of microfibrils into finite-sized fibrils and/or the assembly of fibrils into fibril-bundles.

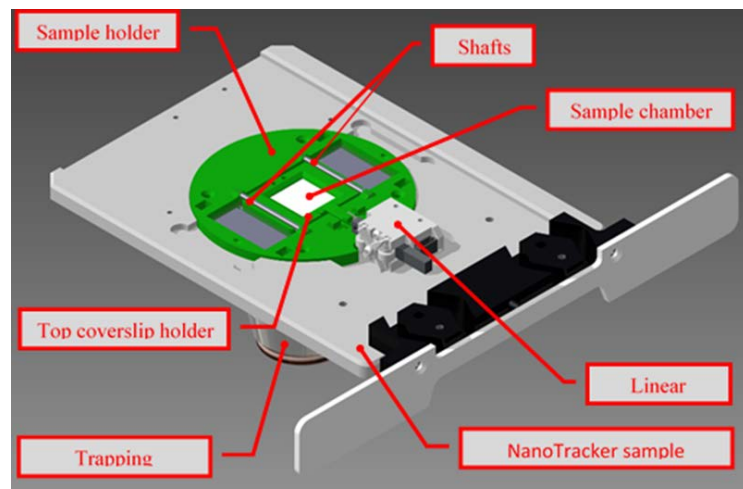
Anisotropic mechanical response of oriented collagen gels

Tissue and tissue scaffolding made from collagen is usually oriented, rather than isotropic. The cells appear to be sensitive to their anisotropic mechanical properties, which we seek here to quantify. Towards this end, we use microrheology to examine the anisotropic fluctuations of Brownian beads embedded in networks that are formed under flow. To impose the flow, we designed and built a small device that could induce flow inside our commercial device for bead tracking and manipulation.

The JPK NanoTracker [2] was used to record thermal fluctuations of 2 μm polystyrene beads (Polybead Polystyrene Microspheres, mean diameter 2.0 μm , standard deviation $\pm 5\%$, Polysciences, Inc., Warrington, PA), embedded into 1 mg/ml self-assembled rat tail type I collagen network (Corning® Collagen I, Rat Tail, Corning Inc., Corning, NY)

To create anisotropy in the sample we used a custom-built device to produce a large amplitude oscillatory shear (LAOS) flow in the sample chamber during the gelation process (Figure 1). The sample (7-8 μl) was placed between microscope coverslips (18x18 mm and 24x55 mm, No1, Thermo Fisher Scientific, Fermont, CA) (Figure 2). The top coverslip was repeatedly moved by a linear motor (PiezoMotor Piezo LEGS® Linear 6N) with an amplitude of 100 μm and maximum speed 10 $\mu\text{m/s}$ during the first 3 hours of

fibrogenesis. To avoid a complicated secondary flow pattern during the shear deformation, only a small



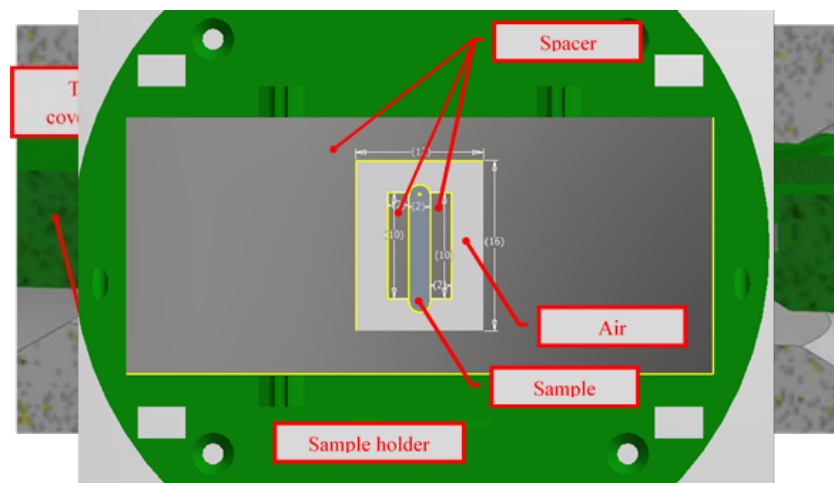
rectangular portion of the sample chamber was actually filled with the sample (Figure 3).

Figure 1 Render of shear chamber.

Figure 2 Shear chamber cross-section

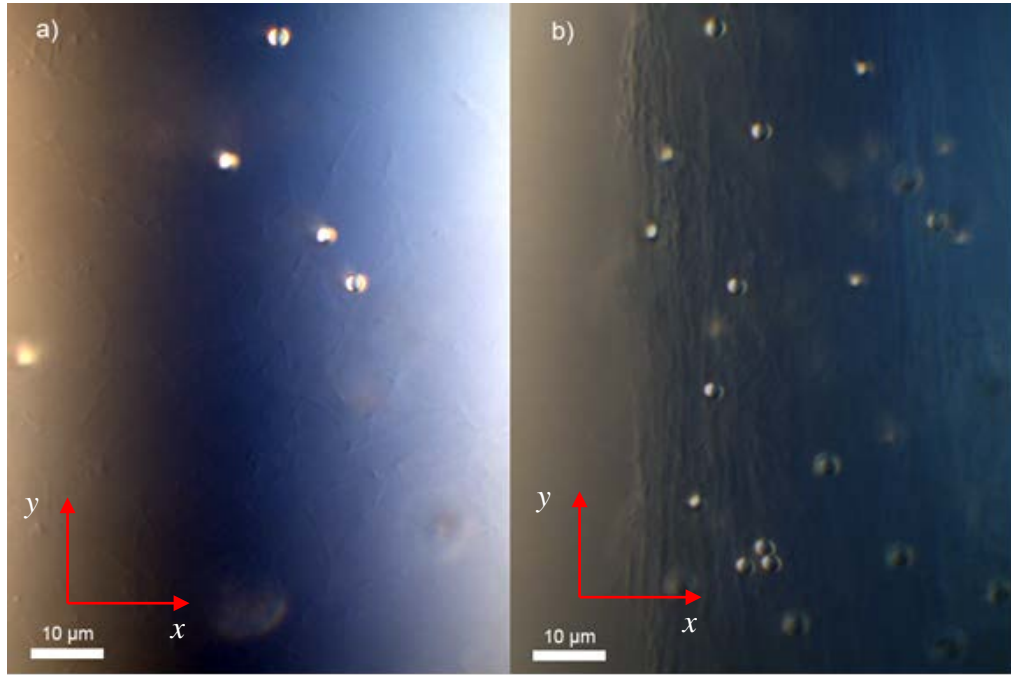
Figure 3 Shear chamber top view (Sizes in mm)

Microrheological experiments were performed as follows. The collagen gel was injected into the sample chamber and left for 3 hours under LAOS flow. An optical trap was focused on the desired bead and calibrated. After that, data of the bead position was collected simultaneously for X and Y channels at the rate of 100 kHz for 60 seconds. Calibration and data collection steps were repeated for 5-10 different beads. The sample chamber was turned 90° counterclockwise and the whole process of the calibration and the data collection was repeated for exactly the same beads. The last step is important for a reproducibility check and for evenly distributing all the internal and external noise sources among X and Y channels.



Results and Discussion

There are two competitive processes occurring in the sample during LAOS. One process is the orientation of fibers along the direction of the shear as described by [3]. The other process caused by LAOS is weakening of the network in the flow direction [4]. As described in [4], the weakening occurs in a mature network due to destruction of cross-linking bounds between fibers. The effect was shown for relatively small oscillatory strains (0.02 – 0.2) and large step strain (0.7) followed by long relaxation time (tens of minutes). However, during fibrogenesis we noticed that cross-links are easily reformed due to the presence of proteoglycans and therefore the fibers are just orient in the direction of LAOS flow (direction along y



axis on Figure 4, b).

Figure 4 Unoriented (a) and oriented (b) collagen networks. For the oriented network (b), the x axis is vorticity direction and the y axis is flow direction.

Observing fibrogenesis under LAOS in real time, we were able to see how newly formed fibers become oriented in the flow direction (y on Figure 4, b) and then bonded to the existing network. Moreover, fibers aggregate in some regions leaving other regions empty. For example, the left side of Figure 4, b is empty of fibers while the middle and right sides contain oriented fiber bundles which are visibly more dense than the unoriented network Figure 4, a.

The mean-square displacement (MSD) of the particle positions on two perpendicular axes (x and y , Figure 4) was calculated for 8 different particles embedded in unoriented (Figure 5 and Figure 6) and oriented (Figure 7 and Figure 8) collagen networks.

One notices significant variance between the MSDs for different particles for both x and y channels. Such variance was reported before [5] and is probably caused by the slight inhomogeneity within the formed fiber bundle (right side of Figure 4, b). To avoid inhomogeneity one can try increasing the collagen

concentration. However, higher collagen concentration will lead to significant stiffening of the network, which in turn decreases the amplitude of the particle motion, possibly to the resolution limit. The latter might be especially important for the oriented networks, which tend to already have higher local collagen concentrations due to the formation of aggregates (bundles).

Comparing MSD plots for x and y channels, one sees that, despite the variation between different particles, the plots look similar. To further analyze the difference between x and y displacements, we plot their relation in Figure 9. For an ideal isotropic network MSD x/MSD y should always equal 1. However, even for our unoriented 1 mg/ml collagen gel there are some deviations from 1. That could be explained by the small concentration of fibers in the gel. Another feature of Figure 9 is that the quantity $\frac{\text{MSD } x}{\text{MSD } y} \xrightarrow{t \rightarrow 0} 1$, which can be explained increased contribution of inertia of the particle and the buffer at high frequencies.

To quantify the anisotropy of the sample, we calculate the average and the standard deviation of MSD x/MSD y for different particles at a lag time of 0.1 s which turned out to be 1.49 ± 0.83 .

Analyzing MSD plots for the oriented network (Figure 7 and Figure 8), one sees that MSDs for the oriented network is generally smaller than for unoriented. This is consistent with the oriented network having higher local collagen concentrations, as was discussed earlier.

Another feature is that plots of MSD y (which correspond to fluctuation of particles along the preferred fiber orientation in bundle on Figure 4, b) for different particles are generally below plots of MSD x for same particles (which correspond to fluctuation of particles perpendicular to the preferred fiber orientation in the bundle on Figure 4, b). This appears to be an effect of anisotropy in the fiber bundles as motion is more restricted in the direction y on Figure 4.

Lastly, a significant amount of noise appears in both Figure 7 and Figure 8. This noise has a distinct spectral signature and is believed to be a result of external vibrations. We took serious efforts in reducing the noise propagated to the samples, but we were only able to reduce it below 10^{-17} m^2 .

To quantify the anisotropy of the oriented sample, we again calculate the average and the standard deviation of MSD x/MSD y for different particles at the lag time of 0.1 s which turned out to be 3.33 ± 1.26 , a clear quantification of anisotropy in the sample.

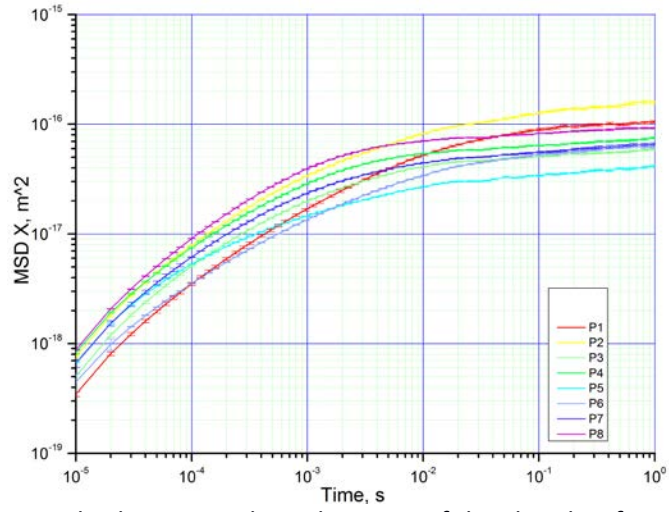
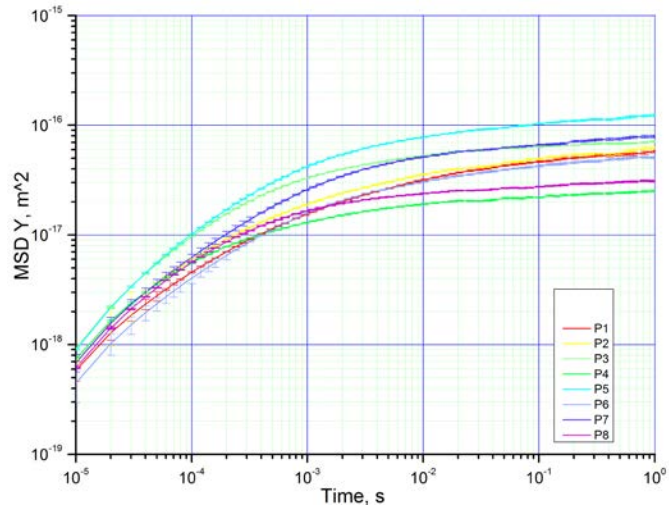


Figure 5 Mean-square displacement along the x axis of the chamber for 8 different particles (P1-P8)



embedded into non-oriented collagen network.

Figure 6 Mean-square displacement along the y axis of the chamber for 8 different particles (P1-P8) embedded into non-oriented collagen network.

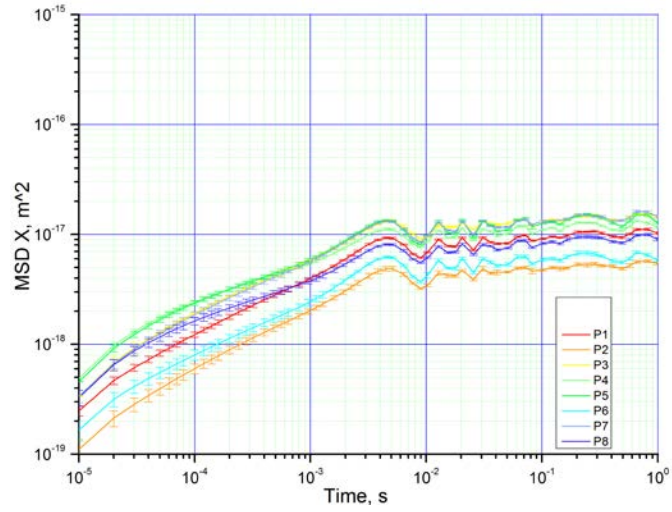


Figure 7 Mean-square displacement along the x axis of the chamber for 8 different particles (P1-P8) embedded into oriented collagen network.

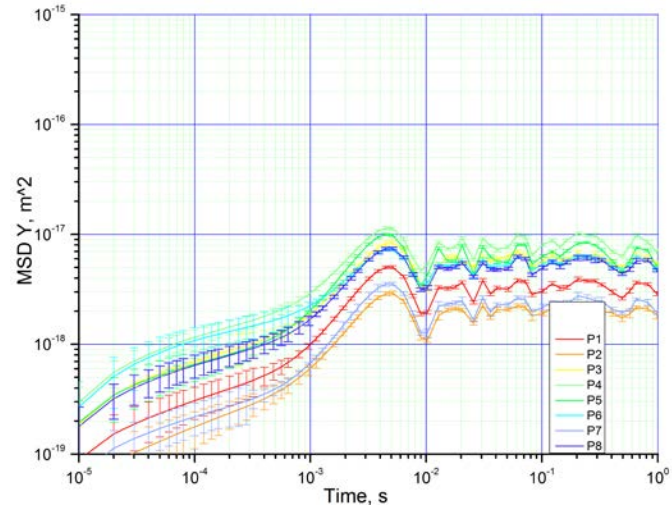


Figure 8 Mean-square displacement along the y axis of the chamber for 8 different particles (P1-P8) embedded into oriented collagen network.

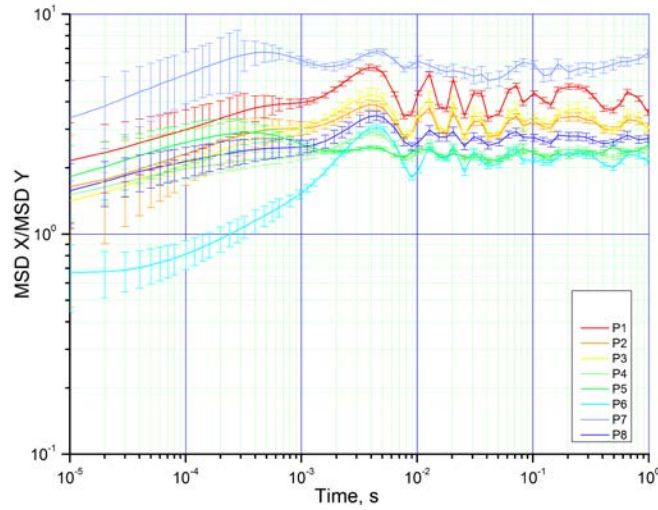
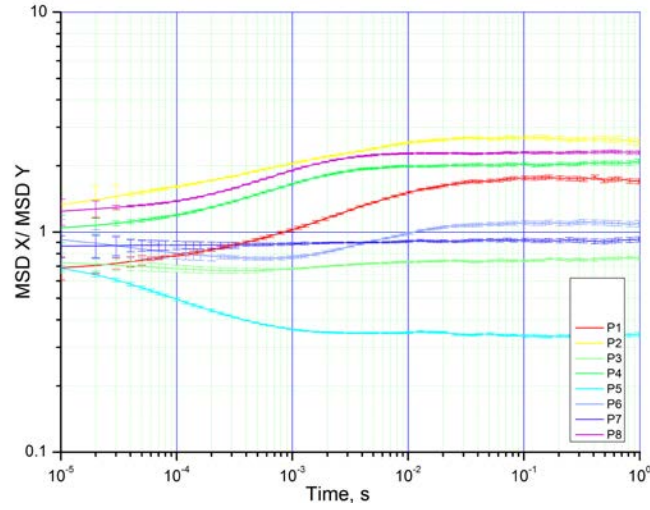


Figure 9 Relation between MSD for x and y displacements ($\text{MSD } x / \text{MSD } y$) for 8 different particles



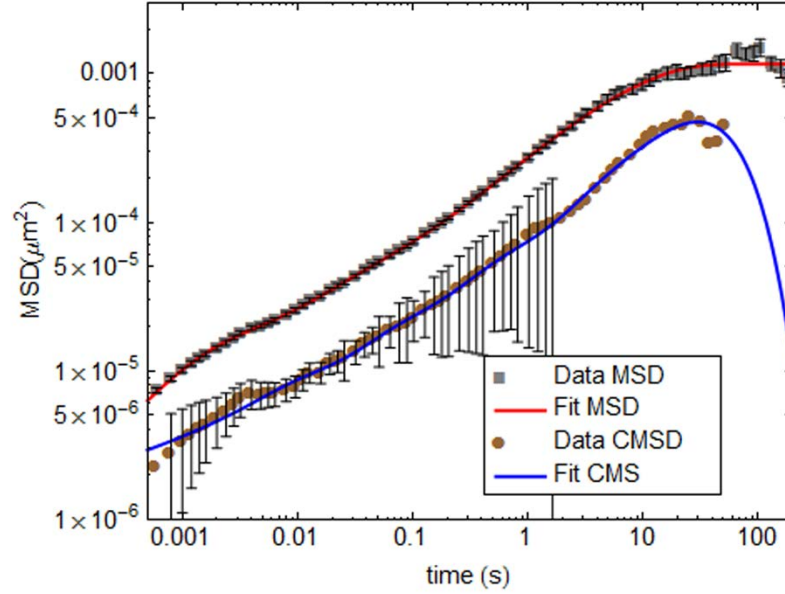
(P1-P8) embedded into non-oriented collagen network.

Figure 10 Relation between MSD for x and y displacements ($\text{MSD } x / \text{MSD } y$) for 8 different particles (P1-P8) embedded into oriented collagen network.

Two-bead microrheology

We have also developed detailed methods for analyzing the results of two-bead microrheology[6]. Roughly speaking, one measures the cross-correlations of the Brownian motion of two beads that interact hydrodynamically in a viscoelastic medium. In single-point microrheology, a single bead is followed, but the bead must be larger than the microstructure of the medium. If the bead is too large, it is not sufficiently subject to Brownian motion, and no signal can be detected. Two-point microrheology overcomes these limitations by using beads that are small enough to experience Brownian forces, but significantly separated to sample the microstructure as a continuum.

Prior analysis neglected two effects: the finite time for waves to travel between the two particles, and the fact that a single wave can bounce between the two particles more than once. We have included these effects and designed an analysis that is no more complicated than the traditional approach [7], [8]. We



apply those analyses here to our own data in a prototype polymer solution, as shown in Figure 11.

Figure 11 Mean-squared displacement, and cross-correlations in two-bead microrheology. The material is 2% PAM(polyacrylamide) dissolved in water. The beads have radius $R = 0.765 \mu m$ and are separated by $4R$. The solid lines are a fit used to convert these data from the time domain to the frequency domain.

These data are then used to estimate the dynamic modulus of the polymer solution and compared to the same quantity measured in a mechanical rheometer. The results are shown in Figure 12.

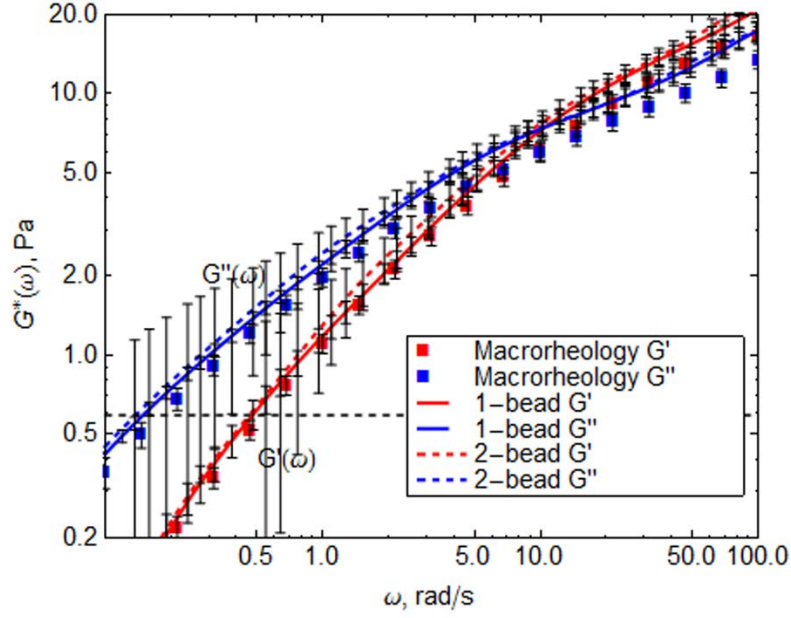


Figure 12 Dynamic modulus measured by a mechanical rheometer in parallel plates (Macrorheology), and that measured using single and two-point microbead rheology.

Semiflexible fiber mechanics

Further coarse graining requires statistical mechanics. Here we model the fibers as fluctuating elastic fibers with uniform Young's modulus, the so-called "wormlike chain" [9]. Great strides were recently made in these derivations and calculations by Spakowitz and coworkers [10]. In order to build mathematical model of networks of these strands, we require the free energy of a strand which interacts with other strands through topological constraints and cross-links. Between these constraints, the strands are relatively free to fluctuate from Brownian forces. However, the strand orientations at these constraints must be continuous, which couples the free energy of two adjacent chain segments.

Using the approach taken by Koslover and Spakowitz [11], we found the Green's function (equivalent to the free energy) of two strands with fixed length (L), fixed end-to-end vector (\mathbf{Q}), and prescribed orientation at their junction (\mathbf{u})

$$\begin{aligned}
 & G(\mathbf{Q}_1, L_1; \mathbf{u}; \mathbf{Q}_2, L_2) \\
 &= \frac{4\pi}{(2\pi)^6} \sum_{n_1} (-1)^{n_1} Y_{n_1}^0(\mathbf{u} \cdot \mathbf{Q}_1 / Q_1, 0) (-i)^{n_1} \int G_{n_1}^{0,0}(k_1; L_1) j_{n_1}(k_1 Q_1) k_1^2 dk_1 \\
 & \sum_{n_2} Y_{n_2}^0(\mathbf{u} \cdot \mathbf{Q}_2 / Q_2, 0) (-i)^{n_2} \int G_{n_2}^{0,0}(k_2; L_2) j_{n_2}(k_2 Q_2) k_2^2 dk_2
 \end{aligned} \tag{1}$$

where the Y are spherical harmonics, the j are spherical Bessel functions, and the $G_n^{0,0}$ are continued fractions.

As an example, we consider the buckling of this strand compared to the prediction of Euler buckling, which does not include fluctuations. Schematic representation of the buckled chain and notations are shown in

Figure 13. Figure 14 shows the critical force required for buckling relative to the Euler prediction. The result shows that fluctuations actually stabilize the fiber. It appears that for short chains, the critical force scales linearly.

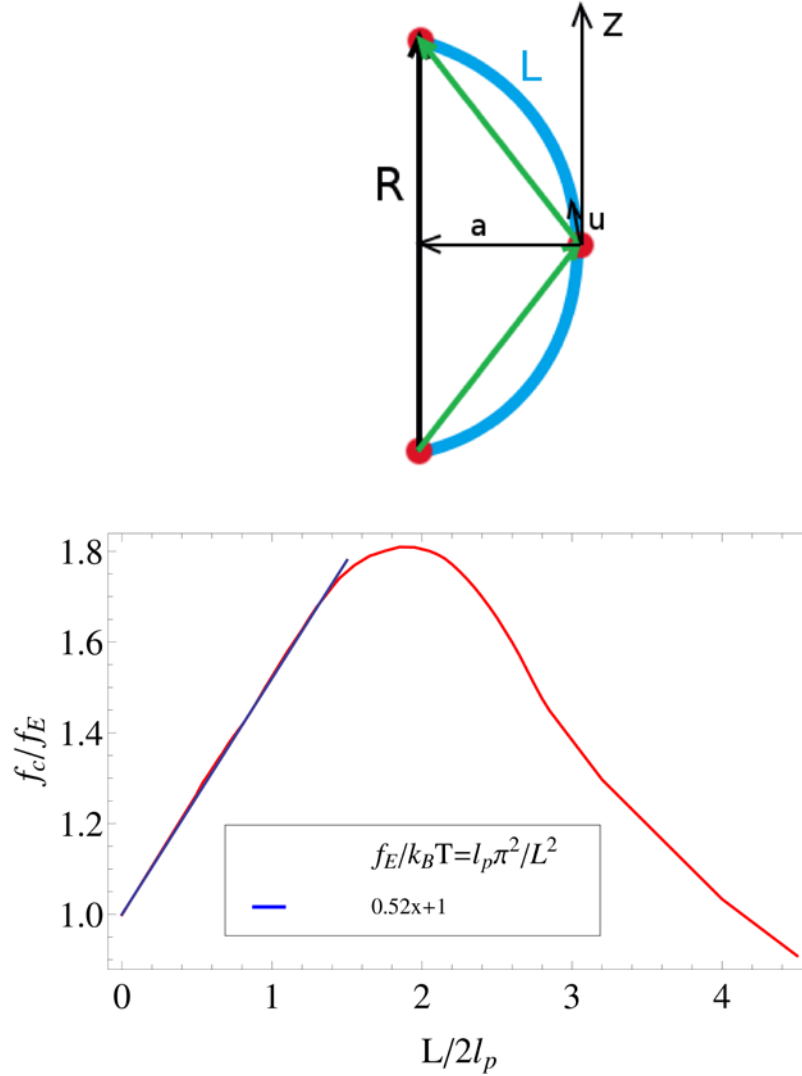


Figure 13 Schematic representation of the chain modeled as 2 equal strands.

Figure 14 Critical buckling force vs contour length of the chain

We also looked at the distribution of the tangent orientation u at the middle of the buckled strand. Examples of this distribution are shown in Figure 15, Figure 16 and Figure 17.

For 10% compression ($R/L = 0.9$) the chain is almost straight and the distribution is sharply peaked at the direction of the end-to-end vector, allowing only small isotropic fluctuation around it (Figure 15). For 50% compression the orientation of the middle point goes out of the plane, indicating that chain configurations can become helical (Figure 16). This suggests that 2D models would not be sufficient to describe buckling of semiflexible fibers, and shows the importance of fluctuations.

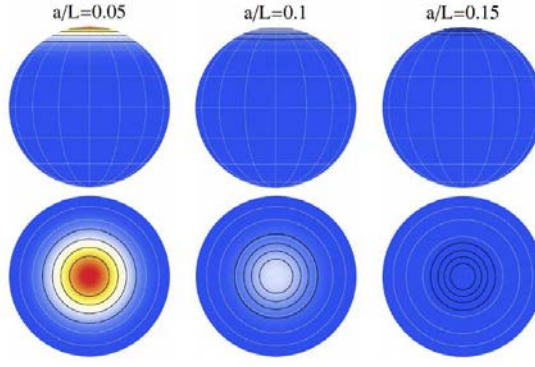
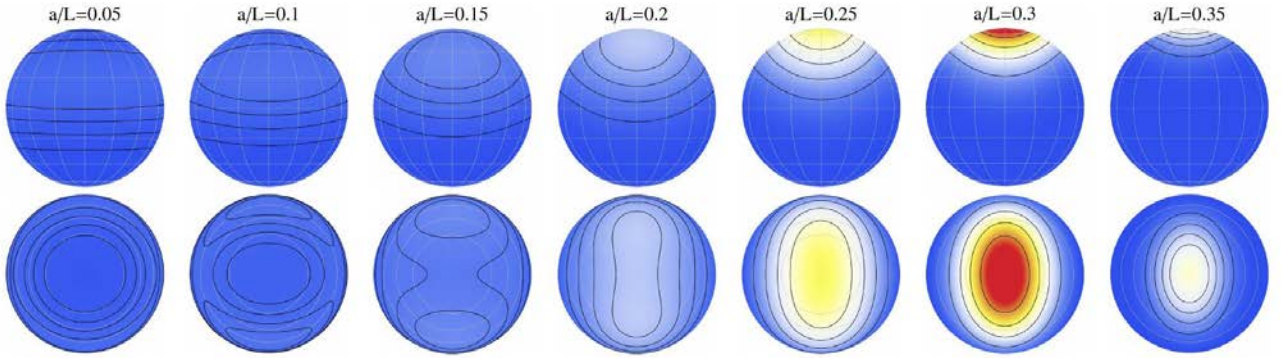


Figure 15 Distribution of orientation angle for the middle point on the chain $L / 2l_p = 2$,



$R / L = 0.9$ ($a_{\max} / L = 0.06$). Color map is the same for all a

Figure 16 Distribution of orientation angle for the middle point on the chain $L / 2l_p = 2$,

$R / L = 0.5$ ($a_{\max} / L = 0.3$). Color map is the same for all a .

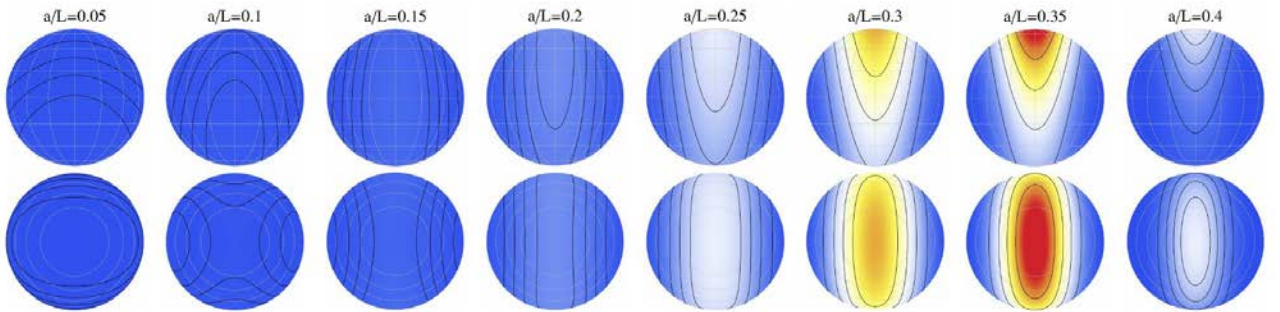


Figure 17 Distribution of orientation angle for the middle point on the chain $L / 2l_p = 2$,

$R / L = 0.1$ ($a_{\max} / L = 0.33$). Color map is the same for all a .

The free energies are then suitable for building multi-chain or single-chain mean-field models of entangled cross-linked semi-flexible networks, such as those that make up tissue.

References

- [1] A. Gautieri, S. Vesentini, A. Redaelli, and M. J. Buehler, "Hierarchical structure and nanomechanics of collagen microfibrils from the atomistic scale up," *Nano Lett.*, vol. 11, no. 2, pp. 757–766, 2011.
- [2] A. Wozniak, J. Van Mameren, and S. Ragana, "Single-Molecule Force Spectroscopy Using the NanoTracker™ Optical Tweezers Platform : from Design to Application," pp. 467–473, 2009.
- [3] I. a. Hasnain and a. M. Donald, "Microrheological characterization of anisotropic materials," *Phys. Rev. E - Stat. Nonlinear, Soft Matter Phys.*, vol. 73, no. 3, p. 031901, Mar. 2006.
- [4] S. Münster, L. M. Jawerth, B. a Leslie, J. I. Weitz, B. Fabry, and D. a Weitz, "Strain history dependence of the nonlinear stress response of fibrin and collagen networks.," *Proc. Natl. Acad. Sci. U. S. A.*, vol. 110, no. 30, pp. 12197–202, Jul. 2013.
- [5] M. Shayegan and N. R. Forde, "Microrheological Characterization of Collagen Systems: From Molecular Solutions to Fibrillar Gels," *PLoS One*, vol. 8, no. 8, p. e70590, Jan. 2013.
- [6] A. Córdoba, T. Indei, and J. D. Schieber, "The effects of compressibility, hydrodynamic interaction and inertia on two-point, passive microrheology of viscoelastic materials," *Soft Matter*, vol. 9, no. 13, p. 3521, 2013.
- [7] A. Córdoba, T. Indei, and J. D. Schieber, "Elimination of inertia from a Generalized Langevin Equation: Applications to microbead rheology modeling and data analysis," *Journal of Rheology*, vol. 56. p. 185, 2012.
- [8] A. Córdoba, J. D. Schieber, and T. Indei, "The effects of hydrodynamic interaction and inertia in determining the high-frequency dynamic modulus of a viscoelastic fluid with two-point passive microrheology," *Phys. Fluids*, vol. 24, no. 7, p. 073103, 2012.
- [9] E. H. Yamakawa, *Modern Theory of Polymer Solutions*. Harper & Row, Publishers, Inc, 1971.
- [10] E. F. Koslover and A. J. Spakowitz, "Systematic Coarse-Graining of Microscale Polymer Models as Effective Elastic Chains," *Macromolecules*, vol. 46, no. 5, pp. 2003–2014, 2013.
- [11] S. Mehraeen, B. Sudhanshu, E. F. Koslover, and A. J. Spakowitz, "End-to-end distribution for a wormlike chain in arbitrary dimensions," *Phys. Rev. E - Stat. Nonlinear, Soft Matter Phys.*, vol. 77, 2008.